BIOCHEMISTRY
including biophysical chemistry & molecular biology

ARTICLE

pubs.acs.org/biochemistry

# Role of Subunit NuoL for Proton Translocation by Respiratory Complex I

Stefan Steimle, Csaba Bajzath,[†] Katerina Dörner, Marius Schulte, Vinzenz Bothe, and Thorsten Friedrich*

Institut für Organische Chemie und Biochemie, Albert-Ludwigs-Universität, Albertstrasse 21, 79104 Freiburg, Germany

Supporting Information

**ABSTRACT:** The NADH:ubiquinone oxidoreductase, respiratory complex I, couples the transfer of electrons from NADH to ubiquinone with a translocation of protons across the membrane. The complex consists of a peripheral arm catalyzing the electron transfer reaction and a membrane arm involved in proton translocation. The recently published X-ray structures of the complex revealed the presence of a unique 110 Å "horizontal" helix aligning the membrane arm. On the basis of this finding, it was proposed that the energy released by the redox reaction is transmitted to the membrane arm via a conformational change in the horizontal helix. The helix corresponds to the C-terminal part of the most distal subunit NuoL. To investigate its role in proton translocation, we characterized the electron transfer and proton translocation activity of complex I variants lacking either NuoL or parts of the C-terminal domain. Our data suggest that the $H^+/2e^-$ stoichiometry of the ΔNuoL variant is 2, indicating a different stoichiometry for proton translocation as proposed from structural data. In addition, the same $H^+/e^-$ stoichiometry is obtained with the variant lacking the C-terminal transmembraneous helix of NuoL, indicating its role in energy transmission.

**Role of subunit NuoL for proton translocation by the respiratory complex I**

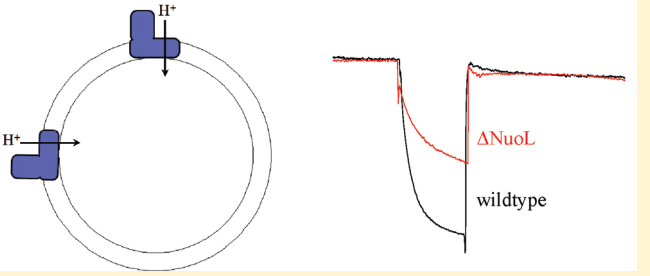


The proton-pumping NADH:ubiquinone oxidoreductase, respiratory complex I, is the main entrance of electrons into the respiratory chains of mitochondria in most eukaryotes and many bacteria. It couples the transfer of two electrons from NADH to ubiquinone with the translocation of four protons across the membrane (current consensus value), thus contributing to the proton motive force used for energy-consuming processes.[1−6]

The bovine complex consists of 45 subunits and has a molecular mass of ∼1 MDa.[7] The bacterial homologues generally consist of 14 subunits that are named NuoA−N (from NADH:ubiquinone oxidoreductase) or Nqo1−14 (from NADH:quinone oxidoreductase). Because of the homology of the subunits, the common cofactor content, and the common catalytic activity, bacterial complex I is regarded as a simpler model for the eukaryotic complex.[8] Electron microscopy revealed the two-part structure of the complex consisting of a peripheral arm protruding into the aqueous phase and a membrane arm buried in the lipid bilayer.[9,10] The peripheral arm contains the NADH binding site and all cofactors, while proton translocation takes place in the membrane arm. The ubiquinone binding site is supposedly located at the interface of the two arms.[11−13]

The structure of the peripheral arm of *Thermus thermophilus* complex I revealed the putative electron pathway from NADH by a chain of seven iron−sulfur (Fe−S) clusters to the ubiquinone binding site.[14,15] However, the coupling of the electron transfer reaction to proton translocation as well as the mechanism of proton translocation is not understood. Most notably, the membrane arm contains three subunits named NuoL, NuoM, and NuoN, which derive from a common ancestor and which are homologues of monovalent cation/$H^+$ antiporters.[4,16,17] It is most reasonable to assume that they are involved in proton translocation. The recently determined structure of complex I from *T. thermophilus* and *Yarrowia lipolytica* revealed that these antiporter-like subunits are located at the most distal position of the membrane arm.[18,19] They consist of 14 transmembraneous (TM) helices each arranged in a core of four central helices surrounded by a ring of 10 residual helices. The latter include two discontinuous TM helices connected by a loop in the membrane. It was proposed that this type of helix is important for ion translocation in transporters.[20] In addition, the structure of the bacterial complex revealed the presence of a 110 Å amphipathic helix aligned parallel to the membrane arm. The same structural element was found in the mitochondrial complex, however, at a length of 60 Å.[19] The amphipathic helix is anchored on both ends of NuoL by two additional TM helices. This unique domain is the C-terminal part of NuoL and conserved within the family of energy-converting hydrogenases and antiporters.[18] It clearly distinguishes NuoL from its homologues, NuoM and NuoN.

**Received:** February 21, 2011
**Revised:** March 17, 2011
**Published:** March 21, 2011

It was proposed that the helix is used as a piston to transmit the energy released by the redox reaction in the peripheral arm to proton translocation in the membrane arm. It is generally assumed that complex I translocates four protons per NADH oxidized across the membrane.[21−23] According to the structure of the bacterial complex, Efremov et al.[18] proposed that by an unknown mechanism the ubiquinone reduction induces a piston-like movement of the amphipathic helix in the membrane arm. Because of this movement, the three antiporter-like subunits, NuoL, NuoM, and NuoN, are opened (and closed), leading to a translocation of one proton by each of the subunits. It is proposed that the fourth proton is translocated at the quinone binding site by another yet unknown mechanism. In contrast, Ohnishi et al.[24] postulated that only two protons are translocated by the antiporter-like subunits.

To investigate the role of the additional C-terminal domain of NuoL in proton translocation and to shed some light on the possible mechanism of proton translocation, we overproduced and isolated variants of the complex either lacking NuoL or containing C-terminally truncated versions of NuoL. All variants revealed inhibitor-sensitive electron transfer activity. After reconstitution in proteoliposomes, they exhibited redox-driven proton translocation but to a reduced extent. From our data, we conclude that there are at least two coupling sites in complex I and that the C-terminal domain of NuoL is essential for the translocation of $2H^+/2e^-$.

## MATERIALS AND METHODS

**Materials and Strains.** A derivative from *Escherichia coli* strain BW25113[25] from which the *nuo* operon had been deleted by genomic replacement methods was used[26] (M. Vranas and T. Friedrich, unpublished results). In addition, *E. coli* strains DH5α[27] (Invitrogen) and DH5αΔ*nuo*[28] and plasmids pCA24N*nuoL*,[29] pUM24,[30] pKD46,[25] and pBAD*nuo*$_{His}$[30] were used in this study. (For a detailed description of strains and plasmids, see Tables S1 and S2 of the Supporting Information.) Ampicillin (100 μg/mL), chloramphenicol (170 μg/mL), and kanamycin (50 μg/mL) were supplemented where necessary. All enzymes used for recombinant DNA techniques were obtained from Fermentas (St. Leon-Roth, Germany) and DNA oligonucleotides from MWG Operon (Ebersberg, Germany) (Table S3 of the Supporting Information).

**Site-Directed Mutagenesis.** Plasmid pCA24N*nuoL*[29] was used to introduce mutations into *nuoL*. Primer pairs pCA_nuoL_Y544Stop and pCA_nuoL_W592Stop (Table S4 of the Supporting Information) were used to create plasmids pCA24N*nuoL*/Y544Stop and pCA24N*nuoL*/W592Stop.

**λ-Red-Mediated Recombination.** Electrocompetent DH5αΔ*nuo*/pKD46 cells were prepared and electroporated as described previously.[28] The *nptIsacRB* cartridge was amplified from pUM24 with the primer pair nuoL_nptIsacRB (Table S3 of the Supporting Information). The *nuoL* gene on pBAD*nuo*$_{His}$ was replaced by the selection cartridge by λ-Red-mediated recombination;[26] 50 μL of electrocompetent cells was mixed with 50 ng of pBAD*nuo*$_{His}$ and 250 ng of the linear DNA fragment. To select recombinants, 200 μL of the cells was plated onto LB agar with kanamycin. Plasmids were isolated from Km$^R$ clones and purified by linearization via *Sac*I restriction. DH5α cells were transformed with the linearized plasmid and grown on LB agar supplemented with kanamycin. The *nptIsacRB* cartridge on pBAD*nuo*$_{His}$ was replaced by a polymerase chain reaction (PCR) product containing the desired mutation in *nuoL* by a second λ-Red-mediated recombination step. For this purpose, a linear DNA fragment was amplified from pCA24N*nuoL* carrying the mutation with the primer pair pCA_nuoL (Table S3 of the Supporting Information). Electrocompetent DH5αΔ*nuo*/pKD46 cells were cotransformed with 50 ng of pBAD*nuo*$_{His}$/*nuoL*::*nptIsacRB* and 100−300 ng of the PCR product. Recombinants were selected on YP agar supplemented with chloramphenicol and 10% (w/v) sucrose at 30 °C. Plasmids from Cam$^R$ and Suc$^R$ clones were isolated. All mutations were confirmed by DNA sequencing (GATC, Konstanz, Germany).

**Isolation of Complex I and the Variants.** The complex and its variants were isolated as described previously.[30] Additional anion exchange chromatography was included to enhance purity. In general, the membrane proteins were extracted using *n*-dodecyl β-D-maltopyranoside (DDM) (AppliChem) and separated by anion exchange chromatography on Fractogel EMD TMAE Hicap (Merck). Fractions with NADH/ferricyanide oxidoreductase activity were pooled and subjected to affinity chromatography on Ni-IDA material (Invitrogen). The column was washed, and bound proteins were eluted in an imidazole gradient.[30] The preparations were further purified on a 15 mL Source 15Q (Amersham Biosciences) column equilibrated in 50 mM MES/NaOH, 50 mM NaCl, and 0.1% DDM (pH 6.0) at a flow rate of 1.5 mL/min. Bound proteins were eluted in a 40 mL linear gradient from 150 to 350 mM NaCl in 50 mM MES/NaOH and 0.1% DDM (pH 6.0). Peak fractions with NADH/ferricyanide oxidoreductase activity were combined and concentrated (Amicon Ultra-15, Millipore, 100 kDa molecular mass cutoff). Typical courses of the preparations are given in Tables S5−S8 of the Supporting Information. The homogeneity of the preparations was analyzed by size exclusion chromatography; 200−300 μg of the preparations was applied to a 26 mL Superose 6 10/300 GL column (GE Healthcare) equilibrated in 50 mM MES/NaOH, 50 mM NaCl, and 0.1% DDM (pH 6.0). The protein was eluted in the same buffer at a flow rate of 0.5 mL/min.

**Electron Transfer Activity.** The physiological NADH:decylubiquinone oxidoreductase activity of the preparations was measured by monitoring the decrease in the NADH concentration at 340 nm using an ε of 6.3 $mM^{-1}$ $cm^{-1}$ (TIDAS II, J&M[31]). The preparations were reconstituted in proteoliposomes as described previously.[31] Proteoliposomes (5 μL) containing 6.5 μg of either complex I or the variants were added to the assay buffer [5 mM MES/NaOH, 50 mM KCl, and 2 mM $MgCl_2$ (pH 6.0)] at 30 °C. The final concentration of the enzyme was 1.3 μg/mL. Decyl-ubiquinone (60 μM) was added, and the assay was incubated for 1 min. The reaction was started via addition of 150 μM NADH.

**Proton Translocation Activity.** The generation of a proton gradient was determined by monitoring the fluorescence quenching of 9-amino-6-chloro-2-methoxyacridine (ACMA, Sigma). Proteoliposomes (5 μL) with 6.5 μg of complex I, 0.2 μM ACMA, and 60 μM decyl-ubiquinone (Sigma) were added to the assay buffer [5 mM MES/NaOH, 50 mM KCl, and 2 mM $MgCl_2$ (pH 6.0)] at 30 °C and incubated for 1 min. The fluorescence was detected with an LS 45 luminescence spectrometer (Perkin-Elmer) at an excitation wavelength of 430 nm and an emission wavelength of 480 nm. The reaction was started via addition of 150 μM NADH (Roth).

**EPR Spectroscopy.** EPR measurements were taken with a Bruker EMX 1/6 spectrometer operating at X-band (9.2 GHz).

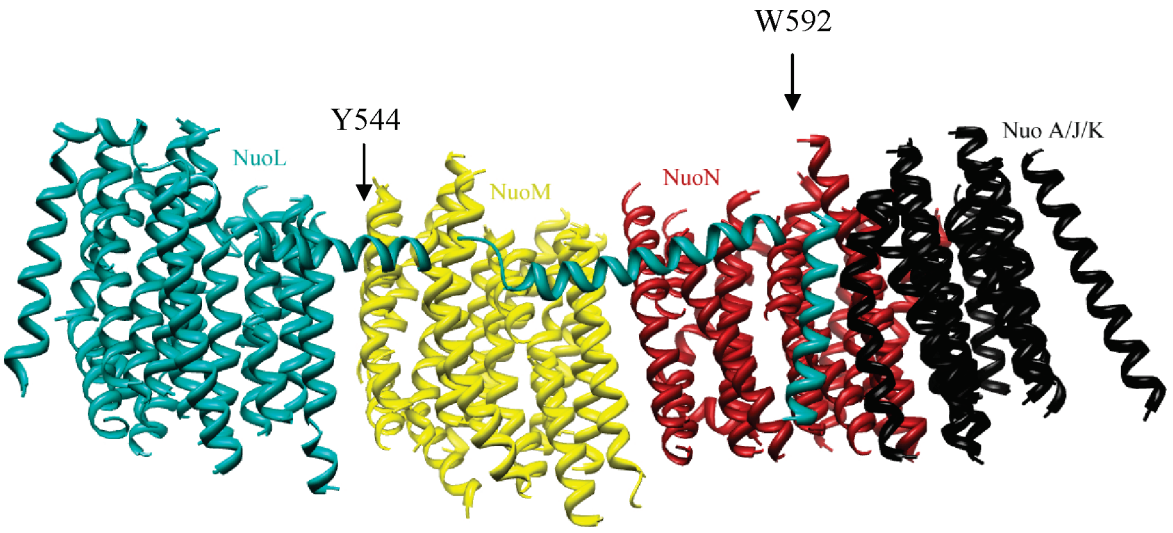


**Figure 1.** Positions of the truncations inserted into the amphipathic helix of NuoL (green-blue). The side view of the membrane arm of *E. coli* complex I (Protein Data Bank entry 3M9C) is shown. The approximate positions of the amino acid residues replaced by a stop codon are denoted with an arrow.

The sample temperature was controlled with an Oxford instrument ESR-9 helium flow cryostat. The preparations (1.5−3 mg/mL) were reduced with a 1000-fold molar excess of NADH and frozen at −78 °C as described previously.[30]

**Other Analytical Procedures.** NADH/ferricyanide oxidoreductase activity was measured as the decrease in absorbance at 410 nm using an $\varepsilon$ of 1 $mM^{-1}$ $cm^{-1}$.[32] The measurements were performed at room temperature with an Ultrospec 1100 *pro* spectrophotometer (Pharmacia) in 50 mM MES/NaOH and 50 mM NaCl (pH 6.0) supplemented with 0.2 mM NADH. The reaction was started via addition of 5 $\mu$L of the protein sample. Protein concentrations were determined by the Biuret method using BSA as a standard. The concentration of purified complex I was determined by the absorbance at 280 nm minus that at 310 nm (TIDAS II, J&M) using an $\varepsilon$ of 763 $mM^{-1}$ $cm^{-1}$ for fully assembled complex I and 665 $mM^{-1}$ $cm^{-1}$ for the ΔNuoL variant as derived from the amino acid sequence.[33] Sodium dodecyl sulfate−polyacrylamide gel electrophoresis (SDS−PAGE) was performed as described previously[34] using a 3.9% stacking gel and a 10% separating gel. Mass spectrometric analysis was conducted at the Zentrum für Biosystemanalyse, Albert-Ludwigs-Universität, with a Q-TOF mass spectrometer (Agilent 6520, Agilent Technologies).

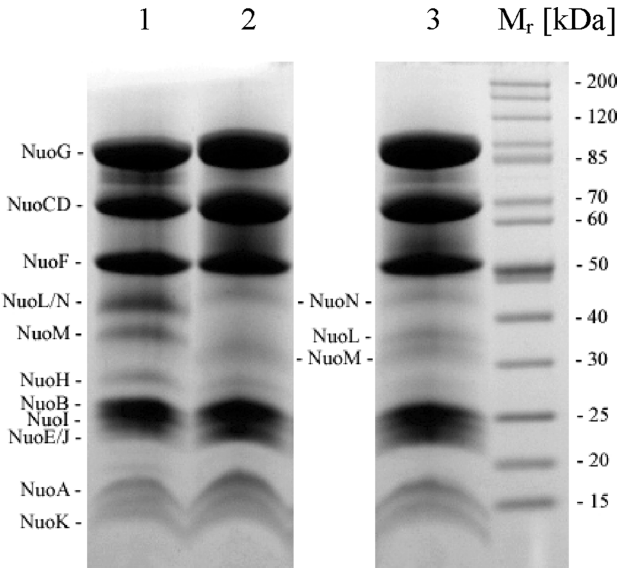


**Figure 2.** SDS−PAGE of the preparations. The wild type was in lane 1, the ΔNuoL variant in lane 2, and the Y544Stop variant in lane 3. The positions of subunits NuoL, NuoM, and NuoN identified by mass spectrometry are indicated.

## RESULTS

**Generation of Mutants.** The 21 kb expression plasmid pBAD*nuo*$_{His}$ containing all 13 *E. coli nuo* genes under the control of the inducible $P_{ara}$ promotor is too large for site-directed mutagenesis. Therefore, the 6 kb plasmid pCA24N*nuoL* containing only *nuoL* was mutated and introduced into the expression plasmid. First, *nuoL* on pBAD*nuo*$_{His}$ was replaced by the *nptIsacRB* selection cartidge via λ-Red-mediated recombination. To prevent unwanted crossover recombination with the chromosomal *nuo* genes, chromosomal deletion strain DH5αΔ*nuo* was used for recombineering. Plasmid pBAD*nuo*$_{His}$/*nuoL*::*nptIsacRB* was used for the overproduction of the ΔNuoL variant. In a second recombination step, the selection cartridge was replaced with a linear DNA fragment containing the mutated version of *nuoL*, which was amplified from subclone pCA24N*nuoL*. The NuoL variants Y544Stop and W592Stop contain a stop codon leading to truncations in the middle and at the end of the horizontal helix (Figure 1). As a result, the W592Stop variant is missing the C-terminal TM helix and the Y544Stop variant is missing this helix and approximately half of the amphipathic helix (Figure 1). Expression strain BW25113Δ*nuo* was transformed with the expression plasmids. The chromosomal *nuo* deletion ensured that the mutant strains contained only the episomal variant of complex I.

**Isolation of the Parental Complex and the Variants.** The parental complex and its variants were isolated from the corresponding strains by affinity chromatography and two anion exchange chromatographies. The complex and the variants eluted at 290 mM NaCl after the first anion exchange chromatography step, at 380 mM imidazole via affinity chromatography,

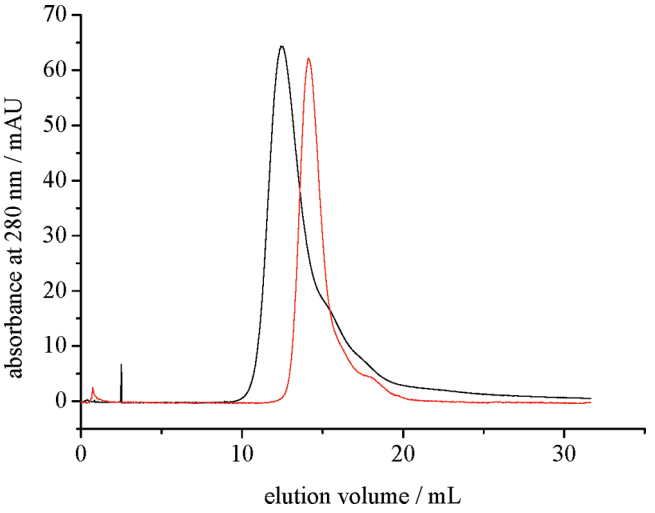


**Figure 3.** Analytical size exclusion chromatography of the preparations of complex I (black) and the ΔNuoL variant (red).

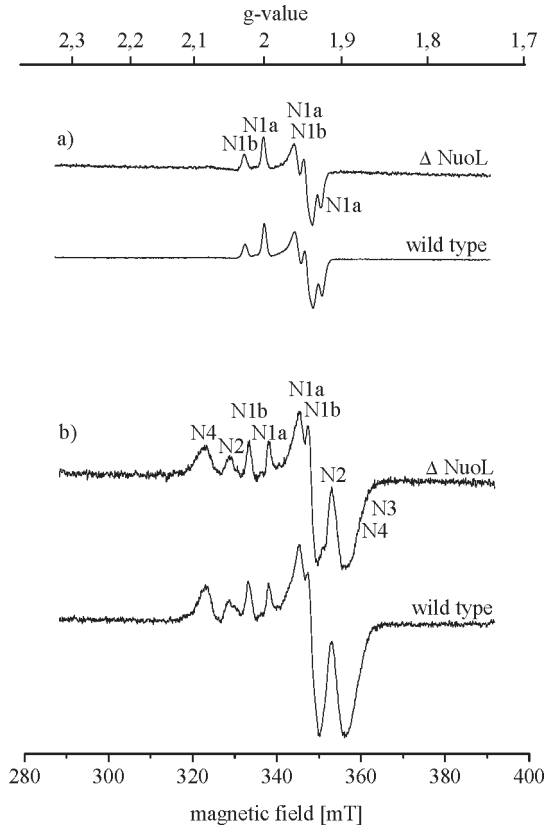


**Figure 4.** EPR spectra of complex I and the ΔNuoL variant. Panel a shows the spectra recorded at 40 K and 2 mW and panel b those recorded at 13 K and 5 mW. The signals are attributed to the individual Fe−S clusters (nomenclature of Ohnishi). Other EPR conditions were as follows: microwave frequency, 9.462 GHz; modulation amplitude, 0.6 mT; time constant, 0.164 s; scan rate, 17.85 mT/min.

and at 190 mM NaCl after the second anion exchange chromatography step. From 30 g of cells, 7 mg of complex I, 5−6 mg of ΔNuoL and the Y544Stop variant, and 2 mg of the W592Stop variant were obtained (Tables S5−S8 of the Supporting Information).

**Table 1. NADH:Decyl-ubiquinone Oxidoreductase and Proton Translocation Activity of Complex I and Several NuoL Variants after Reconstitution in Proteoliposomes**[a]

| proteoliposome contents | NADH:decyl-ubiquinone oxidoreductase activity ($\mu$mol min$^{-1}$ mg$^{-1}$) | ACMA fluorescence quenching (%) |
|---|---|---|
| complex I | 1.5 ± 0.2 (5) | 40 ± 5 (5) |
| ΔNuoL | 1.2 ± 0.2 (5) | 18 ± 3 (5) |
| W592Stop | 1.3 ± 0.2 (2) | 14 ± 2 (2) |
| Y544Stop | 1.2 ± 0.1 (4) | 12 ± 2 (4) |

[a] Each reaction was started by the addition of 150 $\mu$M NADH. The number of preparations from which the standard deviation was calculated is given in parentheses.

SDS−PAGE of the preparation of the parental complex revealed the presence of all subunits of complex I (Figure 2). The presence of NuoL was demonstrated by mass spectrometry of bands extracted from the gel after tryptic digestion as indicated in Figure 2. The preparation of the ΔNuoL variant contained all subunits except NuoL. We were not able to detect a sequence compatible with NuoL in any of the tryptic digests of slices of the corresponding gel by mass spectrometry. The preparations of the variants with a C-terminally truncated NuoL contained the subunit as demonstrated by mass spectrometry of tryptic digests (Figure 2). The truncations in NuoL obviously led to an increased level of binding of SDS per milligram of NuoL as the short forms of NuoL show a lower apparent molecular mass as expected from the mass deduced from the sequence. The apparent molecular masses of the truncated versions of NuoL were similar to that of NuoM.

The homogeneity and the stability of the preparations were demonstrated by analytical size exclusion chromatography (Figure 3). Complex I eluted as a single peak after 12.5 mL and the ΔNuoL variant after 14 mL, which is consistent with its lower molecular mass. Both peaks show a similar shape with some end tailing. The preparations of the variants with C-terminally truncated NuoL eluted with a nearly identical profile after 12.7 mL.

**EPR Spectroscopy.** The Fe−S cluster content of the preparations was analyzed by EPR spectroscopy (Figure 4). The signals of binuclear Fe−S clusters N1a ($g_x$ = 1.92, $g_y$ = 1.94, and $g_z$ = 2.00) and N1b ($g_{\|}$ = 2.03, and $g_{\perp}$ = 1.94) were detected at 40 K in all preparations. In addition, the signals of tetranuclear Fe−S clusters N2 ($g_{\|}$ = 1.91, and $g_{\perp}$ = 2.05), N3 ($g_x$ = 1.88, $g_y$ = 1.92, and $g_z$ = 2.04), and N4 ($g_x$ = 1.89, $g_y$ = 1.93, and $g_z$ = 2.09) were detected at 13 K. Thus, the preparations contained all EPR-detectable Fe−S clusters with identical spectral parameters.

**Electron Transfer and Proton Translocation Activity.** The physiological NADH:decyl-ubiquinone oxidoreductase activity of complex I, the ΔNuoL variant, and the two Stop variants was measured after reconstitution of the preparations in proteoliposomes (Table 1). In total, 80% of the protein added to the reconstitution assay was found in the proteoliposomes for all preparations. The orientation of the reconstituted proteins in the proteoliposomes was determined by measuring the NADH/ferricyanide oxidoreductase activity of the proteoliposomes before and after incubation with 0.5% DDM for 10 min.[31] Approximately half of all preparations were oriented as right-side-out vesicles, while the other half resulted in inside-out vesicles.

In the presence of 150 $\mu$M NADH and 60 $\mu$M decyl-ubiquinone, the parental complex exhibited an electron transfer

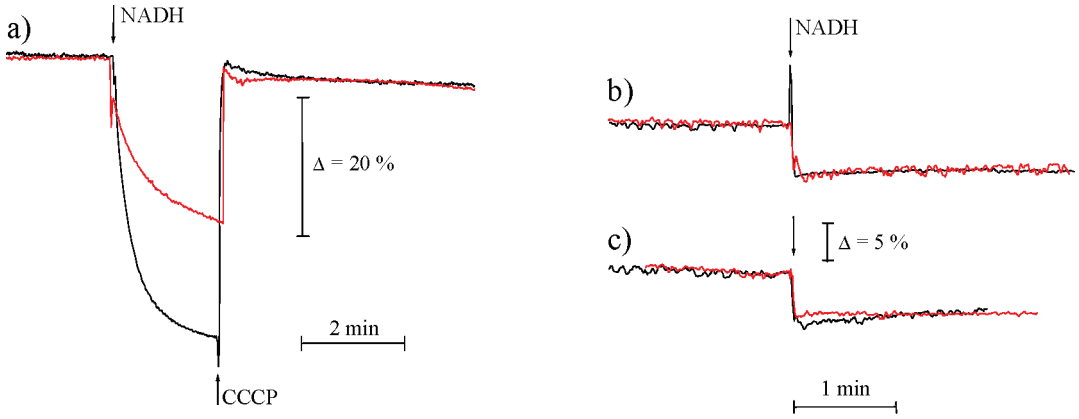


**Figure 5.** Proton translocation by complex I (black) and the ΔNuoL variant (red) after reconstitution in proteoliposomes. The quench of the ACMA fluorescence was measured after the reaction had been started with NADH (a, arrow). The quenching was completely sensitive to an addition of CCCP (a, arrow). Incubation of the proteoliposomes with either CCCP (b) or piericidin A (c) prevented fluorescence quenching.

rate of 1.5 $\mu$mol min$^{-1}$ mg$^{-1}$. The activity of the ΔNuoL variant was determined to be 1.2 $\mu$mol min$^{-1}$ mg$^{-1}$ under the same experimental conditions, which is 80% of the parental activity. Both activities were inhibited to 90% by the complex I specific inhibitor piericidin A. The W592Stop variant and the Y544Stop variant exhibited inhibitor-sensitive electron transfer rates of 1.3 and 1.2 $\mu$mol min$^{-1}$ mg$^{-1}$, respectively (Table 1).

An aliquot of the proteoliposomes used for the electron transfer activity measurement was used to determine the generation of a proton gradient by measuring the quench of the ACMA fluorescence (Table 1 and Figure 5). The addition of 150 $\mu$M NADH to complex I proteoliposomes incubated with 60 $\mu$M decyl-ubiquinone led to a 40% fluorescence quench. Proteoliposomes containing the preparation of the ΔNuoL variant quenched the ACMA signal by 18%. The signals were fully sensitive to CCCP and piericidin A (Figure 5), demonstrating that they derive from a proton gradient generated by the redox reaction of complex I. The proteoliposomes containing the Y544Stop variant and the W592Stop variant were also used for measuring proton translocation activity. The redox reaction of the Y544Stop and W592Stop variants quenched the ACMA fluorescence by approximately 15% (Table 1 and Figure 6).

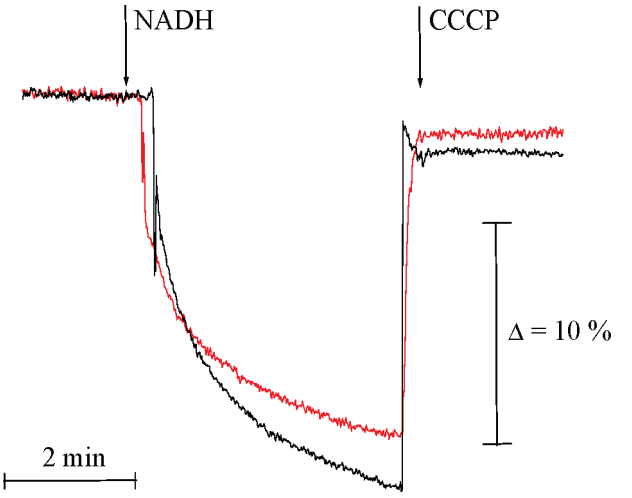


**Figure 6.** Proton translocation by the W592Stop variant (black) and the Y544Stop variant (red) after reconstitution in proteoliposomes. The reaction was started by an addition of NADH, and the proton gradient dissipated after the addition of CCCP.

## DISCUSSION

The type(s) of coupling sites connecting the electron transfer reaction with proton translocation in complex I as well as their number is still unknown. The presence of an either redox-driven[35] or conformationally driven[36] coupling site was proposed. Our group and that of Sazanov and co-workers proposed a mixed mechanism that included both types of coupling sites.[4,15] The importance of the quinone chemistry for proton translocation has been addressed several times.[35,37−39] From the recently published structure of the *T. thermophilus* complex, the presence of a coupling site related to the quinone reduction in a still unknown manner and a series of three conformationally driven coupling sites were proposed.[18] Thus, the data derived from the structure hint at a mixed mechanism of proton translocation. The contribution of the individual coupling sites to the translocation of $4H^+/2e^-$ has so far not been determined experimentally, although it was proposed that direct coupling driven by the quinone chemistry contributes to the translocation of one and indirect coupling to the translocation of three protons per two electrons.[18]

To determine the role of the C-terminal domain of NuoL for proton translocation by complex I, we characterized variants either lacking the C-terminal helix (W592Stop), lacking this helix and approximately half of the amphipathic helix (Y544Stop), or lacking the entire subunit NuoL (ΔNuoL). The variants were produced with an overproduction system recently established in our laboratory allowing protein purification via an affinity tag.[30] All preparations were pure and stable and contained the expected protein composition derived via SDS−PAGE in combination with mass spectrometry. It was not unexpected to obtain fully assembled and structurally intact ΔNuoL variants of *E. coli* complex I because it was shown that NuoL can be selectively removed from the complex by changing the detergent to diheptanoyl-*sn*-glycero-3-phosphocholine without decreasing the stability of the residual complex.[40]

After the reconstitution in proteoliposomes, the ΔNuoL variant exhibited 80% of the electron transfer activity of the parental complex (Table 1). This activity was fully sensitive to piericidin A as was the parental complex. These data indicate that the loss of NuoL has an only very mild effect on the electron transfer activity. This was expected because of the distal location

of this subunit within the membrane arm. However, as the long horizontal helix of NuoL folds back from the most distal position of the membrane arm to the interface between the two arms, its C-terminal helix is within 40−50 Å of the proposed quinone binding site. Apparently, the loss of the C-terminal helix and the loss of the long amphipathic helix of NuoL also have an only very mild influence on the binding and reduction of the quinone. The inhibitor-sensitive NADH:decyl-ubiquinone oxidoreductase activity of the Stop variants was 85% of that of the parental complex (Table 1).

Aliquots of the proteoliposomes were examined for their ability to translocate protons across the membrane. Proton translocation was assayed by ACMA quenching, allowing an only qualitative interpretation of the data. Assuming that the parental complex has a $H^+/2e^-$ stoichiometry of 4,[21−23] our data indicate that the ΔNuoL variant exhibits a $H^+/2e^-$ stoichiometry of 2.2. Not all right-side-out proteoliposomes are tightly coupled and give rise to the quenching of the ACMA signal. Nevertheless, these proteoliposomes contribute to the measured electron transfer activity. Because the preparations were obtained from identical protocols and because the proteoliposomes were made under identical conditions, we assume that the error in the determination of the pH gradient is similar in all samples. Our data indicate that NuoL is most likely involved in the translocation of two protons and not of three as proposed.[18] If the mechanism proposed from the structural data is correct, the ΔNuoL variant should be able to translocate $1H^+/2e^-$. However, the experimentally determined value of $2.2H^+/2e^-$ is closer to the value of $2H^+/2e^-$ proposed by Ohnishi et al.[24] According to this proposal, NuoN is not involved in proton translocation because mutations of conserved charged residues within the subunit had no effect on proton translocation.[41] This is further substantiated by the finding that in higher metazoans the three N-terminal helices of NuoN are missing.[42] On the basis of that, it was proposed that NuoN rather supports the anchoring of the amphipathic helix of NuoL and promotes the coupling of electron transfer with proton translocation.[42] It was also shown that NuoN contains the L-$(X_3)$-H-$(X_2)$-T motif on a cytoplasmic loop.[41] This motif was proposed as a quinone binding motif for respiratory complexes.[43] The assumption that NuoN might be involved in quinone binding is further substantiated by the fact that it is labeled with a photoaffinity analogue of asimicin, a specific quinone site inhibitor of complex I.[44] Thus, according to our data, the three antiporter-like subunits are most likely involved in the translocation of $2H^+/2e^-$. It is proposed that the two residual protons are translocated at the quinone binding site involving the reaction of two different semiquinones.[39]

To investigate the role of the C-terminal domain of NuoL not conserved in its homologues NuoM and NuoN, two stop variants were created. Because the resolution of the complex I model does not allow the identification of individual amino acid residues, suitable positions for the mutations were estimated from sequence comparisons and secondary structure predictions in combination with the structural model (Figure 1). The W592Stop variant missing the C-terminal TM helix and the Y544Stop variant missing this helix and half of the amphipathic helix are capable of proton translocation. Both variants exhibit a stoichiometry of $1.6H^+/2e^-$. This value is lower than that determined for the ΔNuoL variant. The difference could be due to a disordered or flexible arrangement of the amphipathic helix or residual amphipathic helix, respectively, no longer connected to the membrane arm by the C-terminal TM helix of NuoL. In addition, we cannot exclude the possibility that a disordered amphipathic helix within the stop variants allows a random opening and closing of the antiporter-like subunits not coupled with the electron transfer reaction. This scenario would also lead to a decrease in the proton gradient across the membrane.

Nevertheless, the $H^+/2e^-$ stoichiometry of the W592Stop variant missing the C-terminal helix is only slightly reduced to that of the ΔNuoL variant lacking the entire subunit. This stoichiometry is not significantly changed by deletion of half of the amphipathic helix (Y544Stop variant). This shows that the additional C-terminal domain of NuoL is essential for coupling the energy released by the redox reaction within the peripheral arm with proton translocation in the membrane arm. How this transmission takes place on a molecular level has yet to be established. However, our data indicate that the C-terminal TM helix of NuoL is needed to transmit conformational changes from the ubiquinone binding site to the membrane arm.

Taken together, our data indicate that in agreement with the structural data there are at least two different coupling sites for energy conservation in complex I. The reduction of the quinone contributes two protons, and the opening and closing of two of the antiporter-type subunits, most likely NuoL and NuoM, contributes another two protons to the overall stoichiometry of $4H^+/2e^-$ of the complex. For the latter, the presence of the C-terminal TM helix of NuoL is essential.

## ■ ASSOCIATED CONTENT

**Ⓢ Supporting Information.** Strains (Table S1), plasmids (Table S2), oligonucleotides used for λ-Red-mediated recombination (Table S3), oligonucleotides used for site-directed mutagenesis (Table S4), and isolation of complex I and its variants (Tables S5−S8). This material is available free of charge via the Internet at http://pubs.acs.org.

## ■ AUTHOR INFORMATION

### Corresponding Author

*Telephone: +49-(0)761-203-6060. Fax: +49-(0)761-203-6096. E-mail: thorsten.friedrich@uni-freiburg.de.

### Present Addresses

[†]Institut für Physikalische Chemie, Albert-Ludwigs-Universität, Freiburg, Germany.

### Funding Sources

This work is supported by the Deutsche Forschungsgemeinschaft.

## ■ ACKNOWLEDGMENT

We thank Dr. Andreas Schlosser and Stephanie Lamer (ZBSA, Freiburg, Germany) for mass spectrometric analysis, Prof. Dr. Peter Gräber (Institut für Physikalische Chemie, Universität Freiburg, Freiburg, Germany) for access to the luminescence spectrometer, and Linda Williams for her help in correcting the manuscript.

## ■ ABBREVIATIONS

ACMA, 9-amino-6-chloro-2-methoxyacridine; complex I, proton-pumping NADH:ubiquinone oxidoreductase; EPR, electron paramagnetic resonance; FMN, flavin mononucleotide; Fe−S, iron−sulfur; MES, 2-(*N*-morpholino)ethanesulfonic acid; TM, transmembraneous.

## REFERENCES


(1) Weiss, H., Friedrich, T., Hofhaus, G., and Preis, D. (1991) The respiratory-chain NADH dehydrogenase (complex I) of mitochondria. *Eur. J. Biochem. 197*, 563–576.

(2) Walker, J. E. (1992) The NADH:ubiquinone oxidoreductase (complex I) of respiratory chains. *Q. Rev. Biophys. 25*, 253–324.

(3) Ohnishi, T. (1998) Iron-sulfur clusters/semiquinones in complex I. *Biochim. Biophys. Acta 1364*, 186–206.

(4) Friedrich, T. (2001) Complex I: A chimaera of a redox and conformation-driven proton pump? *J. Bioenerg. Biomembr. 33*, 169–177.

(5) Yagi, T., and Matsuno-Yagi, A. (2003) The proton-translocating NADH-quinone oxidoreductase in the respiratory chain: The secret unlocked. *Biochemistry 42*, 2266–2274.

(6) Brandt, U. (2006) Energy converting NADH:quinone oxidoreductase (complex I). *Annu. Rev. Biochem. 75*, 69–92.

(7) Carroll, J., Fearnley, I. M., and Walker, J. E. (2006) Definition of the mitochondrial proteome by measurement of molecular masses of membrane proteins. *Proc. Natl. Acad. Sci. U.S.A. 103*, 16170–16175.

(8) Friedrich, T., and Scheide, D. (2000) The respiratory complex I of bacteria, archaea and eukarya and its module common with membrane-bound multisubunit hydrogenases. *FEBS Lett. 479*, 1–5.

(9) Friedrich, T., and Böttcher, B. (2004) The gross structure of the respiratory complex I: A lego system. *Biochim. Biophys. Acta 1608*, 1–9.

(10) Baranova, E. A., Holt, P. J., and Sazanov, L. A. (2007) Projection structure of the membrane domain of *Escherichia coli* respiratory complex I at 8 Å resolution. *J. Mol. Biol. 366*, 140–154.

(11) Dupuis, A., Prieur, I., and Lunardi, J. (2001) Toward a characterization of the connecting module of complex I. *J. Bioenerg. Biomembr. 33*, 159–168.

(12) Fendel, U., Tocilescu, M. A., Kerscher, S., and Brandt, U. (2008) Exploring the inhibitor binding pocket of respiratory complex I. *Biochim. Biophys. Acta 1777*, 660–665.

(13) Pohl, T., Spatzal, T., Aksoyoglu, M., Schleicher, E., Rostas, A. M., Lay, H., Glessner, U., Boudon, C., Hellwig, P., Weber, S., and Friedrich, T. (2010) Spin labeling of the *Escherichia coli* NADH:ubiquinone oxidoreductase (complex I). *Biochim. Biophys. Acta 1797*, 1894–1900.

(14) Sazanov, L. A., and Hinchliffe, P. (2006) Structure of the hydrophilic domain of respiratory complex I from *Thermus thermophilus*. *Science 311*, 1430–1436.

(15) Berrisford, J. M., and Sazanov, L. A. (2009) Structural basis for the mechanism of respiratory complex I. *J. Biol. Chem. 284*, 29773–29783.

(16) Friedrich, T., and Weiss, H. (1997) Modular evolution of the respiratory NADH:ubiquinone oxidoreductase and the origin of its modules. *J. Theor. Biol. 187*, 529–540.

(17) Mathiesen, C., and Hägerhäll, C. (2002) Transmembrane topology of the NuoL, M and N subunits of NADH:quinone oxidoreductase and their homologues among membrane-bound hydrogenases and bona fide antiporters. *Biochim. Biophys. Acta 1556*, 121–132.

(18) Efremov, R. G., Baradaran, R., and Sazanov, L. A. (2010) The architecture of respiratory complex I. *Nature 465*, 441–445.

(19) Hunte, C., Zickermann, V., and Brandt, U. (2010) Functional modules and structural basis of conformational coupling in mitochondrial complex I. *Science 329*, 448–451.

(20) Screpanti, E., and Hunte, C. (2007) Discontinuous membrane helices in transport proteins and their correlation with function. *J. Struct. Biol. 159*, 261–267.

(21) Wikström, M. (1984) Two protons are pumped from the mitochondrial matrix per electron transferred between NADH and ubiquinone. *FEBS Lett. 169*, 300–304.

(22) Bogachev, A. V., Murtazina, R. A., and Skulachev, V. P. (1996) $H^+/e^-$ stoichiometry for NADH dehydrogenase I and dimethyl sulfoxide reductase in anaerobically grown *Escherichia coli* cells. *J. Bacteriol. 178*, 6233–6237.

(23) Galkin, A., Dröse, S., and Brandt, U. (2006) The proton pumping stoichiometry of purified mitochondrial complex I reconstituted in proteoliposomes. *Biochim. Biophys. Acta 1757*, 1575–1581.

(24) Ohnishi, T., Nakamaru-Ogiso, E., and Ohnishi, S. T. (2010) A new hypothesis on the simultaneous direct and indirect proton pump mechanisms in NADH-quinone oxidoreductase (complex I). *FEBS Lett. 584*, 4131–4137.

(25) Datsenko, K. A., and Wanner, B. L. (2000) One-step inactivation of chromosomal genes in *Escherichia coli* K-12 using PCR products. *Proc. Natl. Acad. Sci. U.S.A. 97*, 6640–6645.

(26) Court, D. L., Sawitzke, J. A., and Thomason, L. C. (2002) Genetic engineering using homologous recombination. *Annu. Rev. Genet. 36*, 361–388.

(27) Hanahan, D. (1983) Studies on transformation of *Escherichia coli* with plasmids. *J. Mol. Biol. 166*, 557–580.

(28) Pohl, T., Bauer, T., Dörner, K., Stolpe, S., Sell, P., Zocher, G., and Friedrich, T. (2007) Iron-sulfur cluster N7 of the NADH:ubiquinone oxidoreductase (complex I) is essential for stability but not involved in electron transfer. *Biochemistry 46*, 6588–6596.

(29) Kitagawa, M., Ara, T., Arifuzzaman, M., Ioka-Nakamichi, T., Inamoto, E., Toyonaga, H., and Mori, H. (2004) Complete set of ORF clones of *Escherichia coli* ASKA library (a complete set of *E. coli* K-12 ORF archive): Unique resources for biological research. *DNA Res. 12*, 291–299.

(30) Pohl, T., Uhlmann, M., Kaufenstein, M., and Friedrich, T. (2007) Lambda Red-mediated mutagenesis and efficient large scale affinity purification of the *Escherichia coli* NADH:ubiquinone oxidoreductase (complex I). *Biochemistry 46*, 10694–10702.

(31) Stolpe, S., and Friedrich, T. (2004) The *Escherichia coli* NADH:ubiquinone oxidoreductase (complex I) is a primary proton pump but may be capable of secondary sodium antiport. *J. Biol. Chem. 279*, 18377–18383.

(32) Friedrich, T., Hofhaus, G., Ise, W., Nehls, U., Schmitz, B., and Weiss, H. (1989) A small isoform of NADH:ubiquinone oxidoreductase (complex I) without mitochondrially encoded subunits is made in chloramphenicol-treated *Neurospora crassa*. *Eur. J. Biochem. 180*, 173–180.

(33) Gill, S. C., and von Hippel, P. H. (1989) Calculation of protein extinction coefficients from amino acid sequence data. *Anal. Biochem. 182*, 319–326.

(34) Schägger, H., and von Jagow, G. (1987) Tricine-sodium dodecyl sulfate-polyacrylamide gel electrophoresis for the separation of proteins in the range from 1 to 100 kDa. *Anal. Biochem. 166*, 368–379.

(35) Brandt, U. (1997) Proton-translocation by membrane-bound NADH:ubiquinone-oxidoreductase (complex I) through redox-gated ligand conduction. *Biochim. Biophys. Acta 1318*, 79–91.

(36) Brandt, U., Kerscher, S., Dröse, S., Zwicker, K., and Zickermann, V. (2003) Proton pumping by NADH:ubiquinone oxidoreductase. A redox driven conformational change mechanism? *FEBS Lett. 545*, 9–17.

(37) Vinogradov, A. D., Sled, V. D., Burbaev, D. S., Grivennikova, V. G., Moroz, I. A., and Ohnishi, T. (1995) Energy-dependent complex I-associated ubisemiquinones in submitochondrial particles. *FEBS Lett. 370*, 83–87.

(38) Yano, T., Magnitsky, S., and Ohnishi, T. (2000) Characterization of the complex I-associated ubisemiquinone species: Toward the understanding of their functional roles in the electron/proton transfer reaction. *Biochim. Biophys. Acta 1459*, 299–304.

(39) Ohnishi, T., and Salerno, J. C. (2005) Conformation-driven and semiquinone-gated proton-pump mechanism in the NADH:ubiquinone oxidoreductase (complex I). *FEBS Lett. 579*, 4555–4561.

(40) Baranova, E. A., Morgan, D. J., and Sazanov, L. A. (2007) Single particle analysis confirms distal location of subunits NuoL and NuoM in *Escherichia coli* complex I. *J. Struct. Biol. 159*, 238–242.

(41) Amarneh, B., and Vik, S. B. (2003) Mutagenesis of subunit N of the *Escherichia coli* complex I. Identification of the initiation codon and the sensitivity of mutants to decylubiquinone. *Biochemistry 42*, 4800–4808.

(42) Birrell, J. A., and Hirst, J. (2010) Truncation of subunit ND2 disrupts the threefold symmetry of the antiporter-like subunits in complex I from higher metazoans. *FEBS Lett. 584*, 4247–4252.

(43) Fisher, N., and Rich, P. R. (2000) A motif for quinone binding sites in respiratory and photosynthetic systems. *J. Mol. Biol. 296*, 1153–1162.

(44) Nakamaru-Ogiso, E., Han, H., Matsuno-Yagi, A., Keinan, E., Sinha, S. C., Yagi, T., and Ohnishi, T. (2010) The ND2 subunit is labeled by a photoaffinity analogue of asimicin, a potent complex I inhibitor. *FEBS Lett. 584*, 883–888.